Strojniški vestnik - Journal of Mechanical Engineering 69(2023)9-10, 388-400
DOI:10.5545/sv-jme.2023.518
Original Scientific Paper
Received for review: 2023-01-05
Received revised form: 2023-05-04
Accepted for publication: 2023-05-30
© 2023 The Authors. CC BY 4.0 Int. Licensee: SV-JME

Mechanical and Microstructural Properties of B_4C/W Reinforced Copper Matrix Composite Using a Friction Stir-Welding Process

Jamuna Elangandhi[1] – Suresh Periyagounder[2] – Mahalingam Selavaraj[3] – Duraisivam Saminatharaja[1]

[1]The Kavery Engineering College, Department of Mechanical Engineering, India
[2]Sona College of Technology (Autonomous), Department of Mechatronics Engineering, India
[2]Sona College of Technology (Autonomous), Department of Mechanical Engineering, India

Copper metal matrix composites (CMC) are broadly employed in various applications in the fields of space, aviation, automobile and electronics industries. The welding of CMC in using conventional methods is very difficult and expensive due to its crystallographic nature. Friction stir welding (FSW) is a more prominent and reliable technique for welding than conventional methods. Therefore, this work is based on work with CMC material, which is prepared with a stir-casting technique. Pure copper (Cu) is reinforced with tungsten (W) and boron carbide (B_4C) particles in different combinations and welded using the FSW process to study the mechanical and micro-structural properties. Multi-objective decision-making methods, such as the technique for order preference by similarity to ideal solution (TOPSIS) and grey relational analysis (GRA) are used to find optimal parameter combination. The experiments are planned according to the L 18 orthogonal array (OA) using the most influential parameters, such as reinforcement the percentage of B_4C, tool rotational speed, welding speed, and axial force. The performance of outcomes is measured based on the responses such as tensile strength, hardness, and impact strength of the weld joint. Based on the results 15 % of B_4C reinforcement, 900 RPM rotational speed, 15 mm/min welding speed and 6 kN axial forces are optimal for better mechanical strength in the welding with TOPSIS and GRA techniques. Additionally, scanning electron microscopic image (SEM) analyses were carried out for better understanding of weldments' microstructure changes.

Keywords: friction stir welding, copper, metal matrix composite, boron carbide

Highlights

- *The CMC materials were produced by the friction stir process and contain pure copper (Cu) as matrix and tungsten (W) and boron carbide (B_4C) as reinforcing material in different concentrations.*
- *Based on experiments with an L-18 orthogonal array (OA), friction stir welding is used to join the CMC cast using parameters such as the percentage of boron carbide reinforcements, tool rotation speed, welding speed and axial force.*
- *The TOPSIS and GRA techniques are used to determine the optimum combination of parameters.*
- *The results of the optimisation show that the mechanical strength when welding with the FSW technique increases with the increase of the reinforcement percentage in the copper composite.*

0 INTRODUCTION

Extensive research attempt has been conducted regarding the FSW process due to its enormous advantages over traditional welding techniques. The FSW process is the most significant and desirable technique in solid-state welding because it is crack-free, fume-free, has less shrinkage and excellent mechanical strength, etc. Also, FSW finds a broad range of utilization in various sectors, such as construction, marine, aircraft, trains, automobile industries and fuel tanks to obtain quality welding of various parts. Although FSW has many reliable features, due to technological growth, it creates new challenges and problems, such as micro-bores, nonhomogeneous welding surfaces, high heat-affected zones, and less mechanical strength of welding. Nevertheless, the needs for CMC in various applications are increasing day by day in the manufacturing sector. Therefore, in view of improving the welding quality of the composite materials, various research attempts have been made in the last decade worldwide.

Zamani et al. [1] carried out experiments with the FSW process on aluminium silicon composite work material and optimized the process parameters using an RSM technique. They planned the design of experiment including the transverse speed of tool and suggested that the optimal process parameter combination was 1300 rpm rotational speed and 70 m/min transverse speed. Moreover, the effect of coupling process parameters increases the machining rate significantly. Argesi et al. [2] attempted to join a pure copper and aluminium alloy with SiC particles in the FSW process. They noted that 50 m/min of welding speed and 1000 rpm of rotational speed produced higher tensile strength. The application of SiC particle increases the hardness of welding strength from 160 HV to 320 HV. Sudhagar and Gopal [3] carried out experiments with FSW to fabricate the surface copper composite using Si_3N_4-reinforced particles in various concentration levels. They

*Corr. Author's Address: The Kavery Engineering College, Department of Mechanical Engineering, India, jamunaelagandhi@gmail.com

analysed the mechanical and microstructure properties of the weld and also observed that while rotating the tool work piece reached recrystallization temperature, which significantly hinders the micro-hardness of welding. The wear property increases with increased reinforcement particles over the surface copper composite by about 15 %. Thapliyal and Mishra [4] utilized the machine-learning concept to weld the copper work material in the FSW process. The most influential parameters (i.e., welding speed, rotational speed and axial forces) are considered for the experiment. They noted a 94 % improved welding strength using this optimal combination among 119 experiments. Harisha et al. [5] welded the copper and aluminium 6083 using the FSW process to study the optimal process parameter combination. They noted a 70 % improved tensile strength in the parameter combination, such as a rotational speed of 1000 rpm and a welding speed of 50 m/min. Nagesh et al. [6] welded dissimilar materials, such as copper and brass, using the FSW process. They compared the results of FSW, such as tensile, hardness, and the impact strength of dissimilar welding strength with parent metal welding, to explore the detailed nature of welding. Senthil et al. [7] studied the FSW process parameters for aluminium 6063 composites using the response surface methodology (RSM) method. They noted the tensile and yield strength of 167 MPa and 145 MPa, respectively, in the parameter value of 1986 rpm of tool speed. Uniform microstructure properties were also noted with the first optimal parameter combination. Karrar et al. [8] studied the effect of tools' rotational and transverse speeds on dissimilar welding in the FSW process. They welded the aluminium alloy 5083 and copper as work material and observed intricate microstructure in the heat-affected zone. Many intermetallic mixers were seen in the welding zone, which leads to nonhomogeneous micro-hardness. The maximum tensile strength was obtained in 1400 rpm tool speed and 120 mm/min. Kolnes et al. [9] prepared a tool for machining materials such as aluminium, copper, and stainless steel, using TiC, and WC-Co-based ceramic composite in the FSW process. The composites are fabricated with a powder metallurgy technique, which prevents the damage caused by the temperature developed through friction. They noted that 80 % of the TiC-mixed composite electrode produces a fine machining surface in the aluminium work material. Sahu et al. [10] investigated the FSW welding characteristics for magnesium work materials. During the welding process, Zn materials are added to improve the welding quality. Also, the addition of Zn with work materials forms an MgZn alloy, which produces high wear strength. Jimenez-Mena et al. [11] attempted a dissimilar weld with materials (e.g., aluminium, steel) using the FSW process. They reported that interlayering of the work material increases when increasing the load application on the work material. Also, the presence of Co in steel increased the toughness of weld and propagated cracks in the aluminium plate. Garg and Bhattacharya [12] carried the welding on aluminium alloys such as 6061 and 7075 using the FSW process. They investigated the mechanical characteristics such as tensile, flexural, and fracture strength of the welding. Copper particles are used during the welding as interference, and 2 mm tool pin is employed in the tool shoulder. Souza et al. [13] carried out experiments in Al-Ce-Si-Mg aluminium alloy using the FSW process. The maximum tensile stress (102 MPa) noted with lesser tool rotational speed using a triangular pin profile surface and higher micro-hardness found at higher rotational speed. Shettigar et al. [14] conducted the experiments in rutile-reinforced aluminium alloy 6061 composite using the FSW process. They planned the experiments with tool, welding speed, and various tool profiles shapes in order to obtain better machining quality. They conducted the experiment so that rotational, transverse speed contributed more to welding accuracy and homogeneous reinforcement distribution among the welding surface. Khojastehnezhad and Pourasl [15] welded the aluminium alloy 6061 with copper through FSW process along with copper particles. They noted defect-less welding in the rotational speed of 950 rpm and 50 mm/min welding speed. The observation shows the welded composite at the edge has higher hardness due to the aluminum and copper bonding. Babu et al. [16] investigated the optimal process parameter for aluminium alloy 2219 with the FSW process to obtain a defect-free machining surface. They used a genetic algorithm to find the possible parameter combination and suggested that a 1005 rpm tool speed at 3º tool angle produces excellent machining performance. This optimization technique diminishes the machining cost significantly due the shorter machining time. Peddavarapu et al. [17] prepared the composite using Al-4.5Cu based alloy and reinforced it with TiB2 particles; this was employed as a work material to study the performance of the FSW process. Normal treaded profile tool was used as tool. They mentioned that uneven material flow, which produces an uneven circumference in the welding. Herbert et al. [18] conducted the experiments in a Cu- and SiC-reinforced aluminium metal matrix

composite, prepared with the stir-casting method and employed in the FSW process to find the optimal welding range of parameters. They used the combined tool profiles (e.g. square and treaded) on the welding and analysed the mechanical and microstructure properties of welding. The hardness of the welding is higher than that of the base metal. Sahu et al. [19] optimized the process parameters of FSW using a fuzzy logic grey analysis method for aluminium and copper welding. They considered the major process parameters, such as tool, welding speed, depth of weld and shape of tool pin. The microstructures of both sides of the metals have fewer defects due to the optimal solution of welding. Ahmadkhaniha et al. [20] carried out the experiments in the FSW process with pure magnesium to find the optimal process parameter combination. They applied the L9 OA and analysed the effect of all parameter combination using the Taguchi method. The harness of magnesium increases with increased tool speed. Shirazi et al. [21] examined the influences of tool and welding speed on the welding strength of aluminium alloy 5456 via the through FSW process. They reported the findings, which showed that, in addition to the optimum parameter, the remaining combinations have a substantial impact on the welding quality. Kumar et al. [22] experimented with aluminium and copper-based composite on the FSW process under various machining speeds and welding speeds. They noted fewer defects with the welding speed in the range of 70 mm/min to 100 mm/min. They also suggest that the microstructure of welding was significantly influenced by the welding and rotational speeds. Suresh et al. [23] studied the influences of various process parameters on the mechanical and microstructure properties of FSW on aluminium alloy 2219 work material using an RSM technique, which was employed to obtain maximum mechanical strength. They found the optimal process parameter combination of1627 rpm rotation speed, 083 mm/s welding speed, and 12.2 kN axial force.

The aforementioned sources were used to explore the optimal solution of FSW process parameters for various aspects, such as aluminium-based composites, copper-reinforced work surfaces, varying concentrations reinforcing particles, and the joining of copper to other metals, such as aluminium, stainless steel, titanium, etc. However, experiments with the copper-based composites and their optimization in the literature are rare [24] to [26] and there is no evidence of hybrid CMC in FSW process. The optimization of the process parameters for every machine is done carefully to achieve the right output without taking major effort. Additionally, optimised values generate high accuracy and reduce unneeded time and cost for quality. In line with that, the TOPSIS and GRA methods are very prominent techniques that are successfully employed in other manufacturing sectors to reveal the optimal solution [27] to [30]. The reinforcement materials, such as W and B_4C particles, provides excellent mechanical strength, thermal stability, and high affinity nature with other materials. Therefore, in this experiment work, material is fabricated with the stir-casting method using commercially available pure copper (Cu) as the matrix and W and B_4C particles as reinforcements in various concentration levels. Based on L18 OA and major influencing parameters, such as the percentage of reinforcements, rotational speed, welding speed, and axial force are used to conduct experiments. The process parameters of FSW are also optimized using simple and prominent techniques, such as TOPSIS and GRA. Furthermore, SEM analyses are carried out on the welding surface to give better understanding of microstructure.

1 EXPERIMENTAL WORK

Commercially available pure copper is considered as the base material, W (30μm), B_4C (50 μm) are employed as reinforcements, and three different CMC materials are fabricated using a stir-casting furnace as shown in Fig. 1. An indigenously created bottom-pouring and electric-stir casting furnace is employed to develop the composite. The Cu rods (25 mm diameter) are cleaned thoroughly and cut into small pieces 10 mm thick. The rods are loaded into a crucible cylinder that is coated with stainless steel and the temperature is maintained at 1200 ºC during the melting process. The molten Cu is stirred well using a stir setup that enhances the distribution of reinforcements uniformly throughout the composite. Stainless steel coating is carried out in the stirrer and crucible, which protects the unwanted material amalgamation with CMC. The preset volume of preheated W and B_4C particles is mixed with the molten copper to enhance the wet ability and mechanical strength with copper material. The weight percentages of reinforcement and composition of composite are displayed in Table 1. The well-mixed molten metal is poured into a die (100 mm × 100 mm × 6 mm) to obtain the hybrid composite.

The fabricated CMC plates are employed to study the weldability using the FSW process. The CMC work material in the plate is fastened with a customized vertical milling machine for the FSW

process. The work plates are arranged in a butt joint design, and the tool is fixed with the tool holder against the workpiece, as shown in Fig. 1.

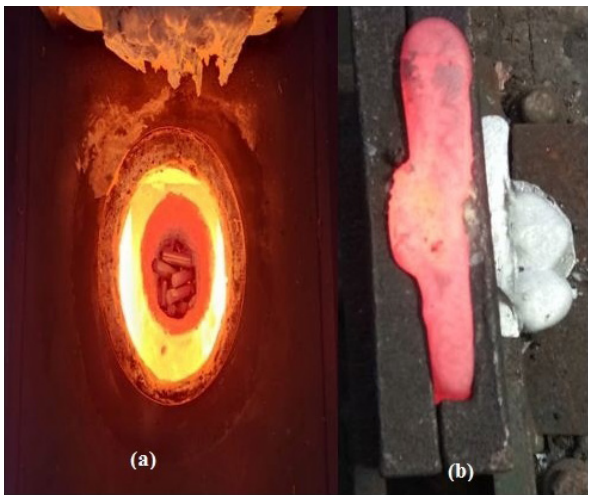

Fig. 1. *Friction stir process; a) casting furnace, and b) casting die with molten CMC*

The non-consumable tool used in the experiment is made of Tungsten carbide with a shoulder diameter of 18 mm. The tool is designed with a hexagon-shape pined with length and diameter of 6 mm and 4 mm, respectively, for the purpose of stirring the work material, as presented in Fig. 2. The rotating tool is plunged over the work material and allowed to rest for 20 seconds to retain its normal temperature. Afterwards, the tool moves over the work material along its length to the weld. Due to the high friction between the tool and electrode, heat is induced, which makes the work materials soften. The shoulder pin of the tool blends the softened work material by moving it from retreating portion to other side which produces a sound weld joint. In this technique, work materials welded using both heat and mechanical energy but in traditional fusion welding only heat energy is employed to weld the metals. The percentage of reinforcements, tool rational speed, welding speed and axial forces influence the welding nature of FSW process. Therefore, these parameters are considered to be input controlling factors. L 18 OA is employed to investigate the process parameter over the output responses. The excellence of welding is evaluated by performing different mechanical and micro-structural testing, including for tensile, impact and hardness. The work materials are sliced into the standard dimensions according to ASTM standard through wire cut EDM. Based on the ASTM E8 standard, test samples are fabricated. Two specimens are cut from every welding specimen and two output responses obtained, which are averaged and considered in order to assess the welding quality. Tables 2 and 3 present the initial parameter levels and design of experiments with output responses respectively, which are considered based on the literature [3]. The micro-hardness of welding is measured using a Vickers hardness testing machine (TE-JINANWDW100, Jinan Test Machine Co. Ltd., China) at different places of welding cross-sections, and average hardness values are considered for evolution. ASTM E23-16a standards are followed to evaluate the impact strength of welding, and a V-notch has been created in welding specimen at right angles to the welding joint.

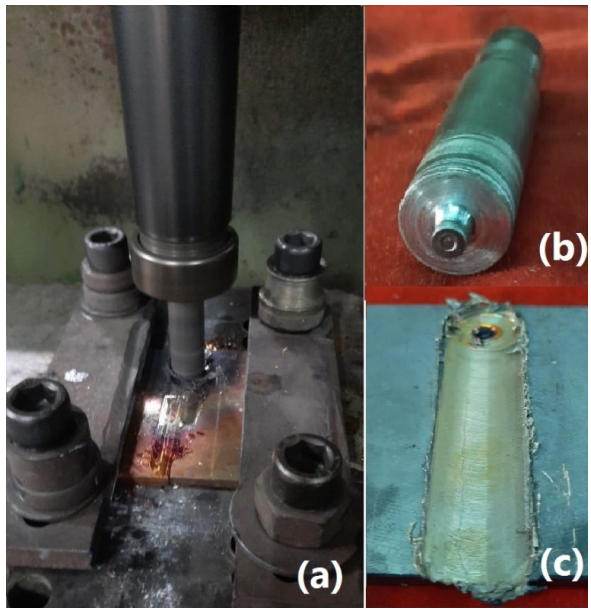

Fig. 2. *Friction stir welding; a) experimental setup, b) tool, and c) work piece*

Table 1. *Composition of CMC*

Plate No.	Symbol	Copper (Cu)	Tungsten (W)	Boron carbide (B_4C)
1	90 % CMC	90	5	5
2	85 % CMC	85	5	10
3	80 % CMC	80	5	15

Table 2. *Input parameter and its levels*

Specimen No.	Parameter	Units	Levels		
			L 1	L 2	L 3
1	Weight % of B_4C	%	5	10	15
2	Rotational speed	rpm	900	1200	1500
3	Welding speed	mm/min	9	12	15
4	Axial force	kN	3	6	9

Table 3. *Design of experiment and output responses*

Experiment No.	Weight % of B_4C	Rotational speed	Welding speed	Axial force	Hardness [HV10]	Tensile strength [N/mm2]	Impact toughness [J]
1	5	900	9	3	83	19.25	3.3
2	5	1200	12	6	91	0.03	3.1
3	5	1500	15	9	45	21.45	3.5
4	10	900	12	9	128	75.455	4.1
5	10	1200	15	3	112	77.75	4.0
6	10	1500	9	6	119	63.821	4.2
7	15	900	15	6	157	22.444	3.9
8	15	1200	9	9	85	136.02	4.0
9	15	1500	12	3	100	153.93	3.8
10	5	900	15	9	82	23.25	2.9
11	5	1200	12	3	89	32.51	3.7
12	5	1500	9	6	59	38.24	3.2
13	10	900	9	9	119	68.25	3.9
14	10	1200	15	3	101	82.57	4.5
15	10	1500	12	6	117	38.14	4.2
16	15	900	15	6	148	120.48	4.5
17	15	1200	12	9	95	125.65	4.2
18	15	1500	9	3	113	148.37	4.9

1.1 Multi Objective Optimization Techniques TOPSIS:

TOPSIS is a popular and very powerful technique to separate the correct parametric mixture from the restricted investigated combination. The steps for this technique are scheduled below. **[27]**

Step 1: The conclusion matrix having 'n' characteristics and 'm' option and it is characterized in Eq. (1).

$$\mathbf{A}_m = \begin{bmatrix} J_{11} & J_{12} & \cdots & J_{1n} \\ J_{21} & J_{22} & \cdots & J_{2n} \\ \vdots & \vdots & \ddots & \vdots \\ J_{m1} & J_{m2} & \cdots & J_{mn} \end{bmatrix}, \tag{1}$$

where J_{ij} is the output of i^{th} option with relevance to the j^{th} characteristic.

Step 2: The normalization of the matrix is carried out with Eq. (2).

$$p_{ij} = \frac{J_{ij}}{\sqrt{\sum_{i=1}^{m} J_{ij}^2}}, \quad j = 1,2,\ldots,n. \tag{2}$$

Step 3: For each output, responses have been assigned with equal weights to be Wt_j ($j = 1,2,\ldots,n$). The standardized weighted choice matrix $\mathbf{M} = [m_{ij}]$ attained using the Eq. (3).

$$\mathbf{M} = Wt_j\, p_{ij}, \tag{3}$$

where $\sum_{j=1}^{n} Wt_j = 1$.

Step 4: The suitable best solution is assessed using Eq. (4) and the worst solution is attained using Eq. (5).

$$M^+ = \left\{\left(\sum_i^{\max} m_{ij} \mid j \in J\right), \left(\sum_i^{\min} m_{ij} \mid j \in J \mid j = 1,\ldots,m\right)\right\} = \left\{m_1^+, m_2^+, .., m_n^+\right\}, \tag{4}$$

$$M^- = \left\{\left(\sum_i^{\min} m_{ij} \mid j \in J\right), \left(\sum_i^{\max} m_{ij} \mid j \in J \mid j = 1,\ldots,m\right)\right\} = \left\{m_1^-, m_2^-, ..., m_n^-\right\}. \tag{5}$$

Step 5: The distributions among every option are intended from the best solutions are obtained using Eq. (6).

$$T_i^+ = \sqrt{\sum_{j=1}^{n} \left(M_{ij} - m_j^+\right)^2}, \quad i = 1,2,\ldots,m. \tag{6}$$

The division of option from the worst solution is attained using Eq. (7).

$$T_i^- = \sqrt{\sum_{j=1}^{n} \left(M_{ij} - m_j^-\right)^2}, \quad i = 1,2,\ldots,m. \tag{7}$$

Step 6: The relations closeness of the dissimilar options for the solutions are obtained using Eq. (8).

$$k_i = \frac{k_i^-}{k_i^+ + k_i^-}, \quad i = 1,2,\ldots,m. \tag{8}$$

Step 7: The k_i standards values are graded in downward order to discover the optimal parameters mixture.

1.2 Grey Relational Analysis Technique

In GRA, output reactions of different elements should be reformed into the dimensionless values. Therefore, those values are standardized to the variety of zero to one using Eqs. (9) to (12) [28]. The tensile, impact, and micro-hardness values must be higher, which considered better and intended using the Eq. (9); for lower, the superior is desirable, which is intended using Eq. (10).

$$R_i^*(s) = \frac{r_i(s) - \min r_i(s)}{\max r_i(s) - \min r_i(s)}, \tag{9}$$

$$r_i^*(s) = \frac{\max r_i(s) - r_i(s)}{\max r_i(s) - \min r_i(s)}, \tag{10}$$

where $i = 1, ,2, \ldots, m$, $s = 1, 2, \ldots, n$, where m is the sum of experiment, n is the sum of the observed data. $R_i^*(s)$ is denoted as minimum - larger than beter and $r_i^*(s)$ as maximum - smaller the better. The standardized values are added in Eq. (11), which is employed to compute the grey relational coefficient (GRC).

$$\lambda_i(S) = \frac{\Delta_{\min} + £\Delta_{\max}}{\Delta_{oi}(P) + £\Delta_{\max}}. \tag{11}$$

Here, $\Delta_{oi}(S)$ divergence series is attained from the orientation series $\lambda_0^*(S)$ and comparability series $\lambda_i^*(S)$. The variety $0 \le £ \le 1$ comprised for the distinctive coefficient:

$$¥ = \frac{1}{n}\sum_{P=1}^{n} £_i(S). \tag{12}$$

Grey relational grade ($¥_i$) is added, summing up of grey relational coefficients which corresponds in Eq. (12). is assisted to discover the connection of situation and comparability ideals.

2 RESULTS AND DISCUSSION

2.1 Effect of Reinforcements on the Microstructure of Welding

SEM is employed to investigate the microstructural properties of the welding joints. The macro-size welding images of various reinforced specimens under different machining conditions are analysed. The microstructure of the welding zone and the parent metal of the welding using various reinforced work materials (e.g., 90 % CMC, 85 % CMC and 80 % CMC) are presented in Figs. 3 to 5. The consistency of welding joint on all sides of the parent metal is found to be better in 80 % CMC materials than other reinforced work materials and lesser regularity found in 90 % CMC material. The microstructures of welding zone for all type of reinforced materials are analysed using SEM images. The SEM analysis shows that the dissemination of grains due to high temperatures enlarges the welding zone on the work material, which could be observed as a bright exterior next to the parent metal. The microstructures of various welding surfaces show that associated coarse grains with consistent grain outlines in a welding zone is attained by means of the elevated heat of the FSW process [20]. Fig. 3 presents the microstructure of welding zone and its field emission scanning electron microscopy (FESEM) image for 90 % CMC work material. In this, 90 % CMC material creates minor non-homogeneous welding on the parent metal; a small number of micro-voids were produced by over welding. Also, the distribution of welding is found to be higher on this CMC work material than others. Welding through 85 % CMC work material creates micro-cracks in the welds and a few granular fractures were observed, which is presented in Fig. 4. The effective diffusion of B_4C, W. and Cu produces extended dendrites in the welding zone which lead to micro-crack structures on the welding. Fig. 5 shows 80 % CMC work material, which provides superior consistent welding zone and a very minor amount of slip microstructure obtained across the welding surface [16]. White impulsive particles are found above the welding surface, which is due to the dispersion of Cu and W materials into the matrix exterior layer of work material. The elevated carbide content in the reinforcement material indicates the prominent oxidation at elevated temperature, which is leads to the development of molten metal on welding zone.

2.2 Micro-hardness

A Vickers micro-hardness test was conducted for various reinforced copper work materials on welding regions; the results of the welding presented in Fig. 6. The graph reveals that the hardness of the 90 % CMC work material is the lowest. The micro-hardness of welding is generally based on the microstructure variations. It is clear from Fig. 6 that the standard hardness of welding formed by 80 % CMC work material is 3.42 % higher than that of welding by 90 % CMC work material. Also, the hardness for 80 %

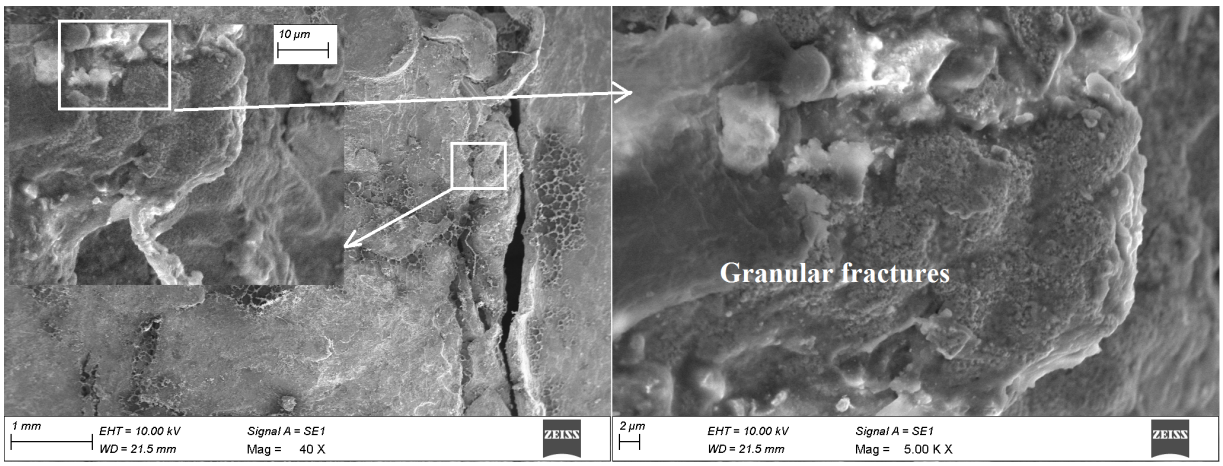

Fig. 3. *SEM image of 90 % CMC welding zone*

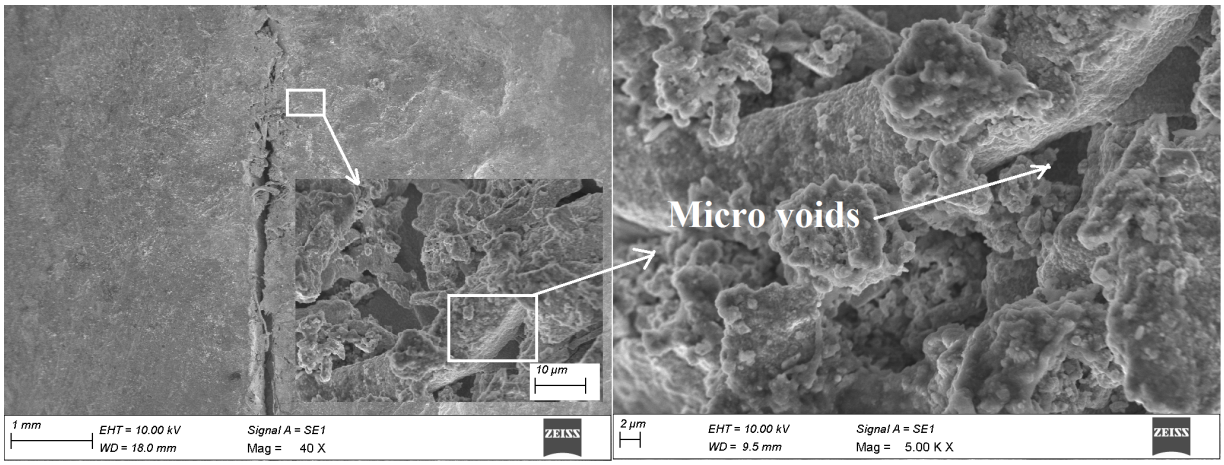

Fig. 4. *SEM image of 85 % CMC welding zone*

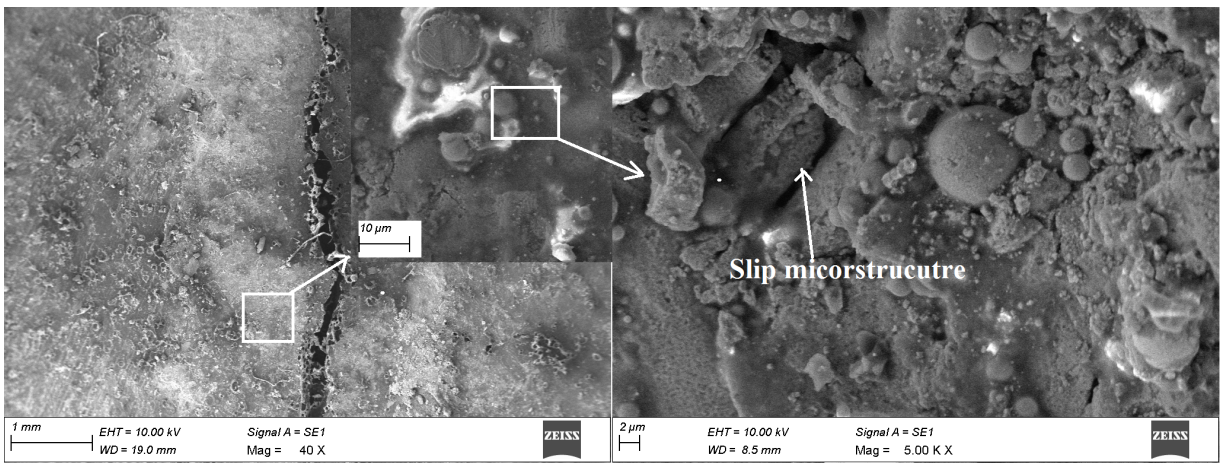

Fig. 5. *SEM image of 80 % CMC welding zone*

CMC work material at parent material is shown to be higher compared to the welding using 90 % CMC work material, due to the enhancement of carbide and W in the parent metal **[20]**. The standard hardness of 80 % CMC work material is 2.8 % more than that of 90 % CMC work material work material. The welding and parent metal hardness are 108 HV and 113 HV, respectively, when 80 % CMC work material. The

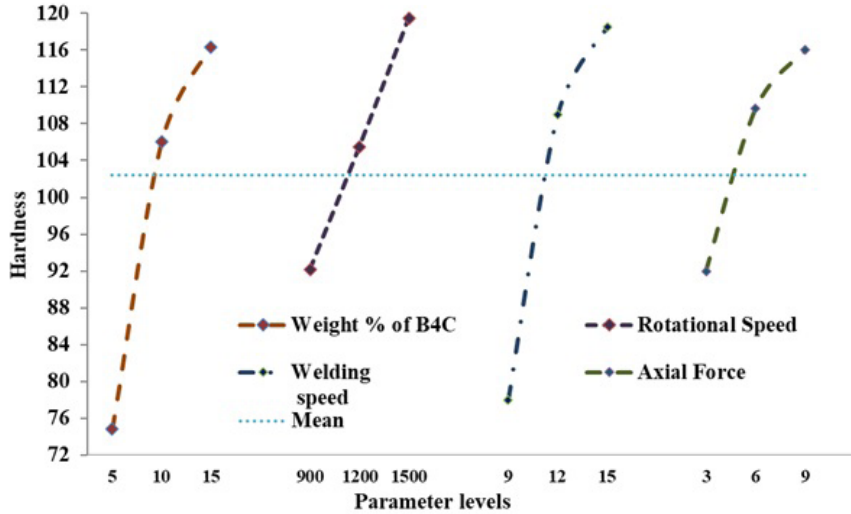

Fig. 6. *Micro-hardness representation*

addition of 15 % B_4C reinforcements on 90 % CMC metal requires more time to melt than 85 % CMC metals that make the microstructure alteration. It is implicit that standard hardness when using of 85 % CMC creates 2.56 % higher hardness compared to 80 % CMC materials. The alteration of cooling rate in welding zone modifies the crystal metal microstructure headed for an austenitic structure [21]. Also, the crystal microstructure is inflated with the increase in temperature, which becomes softer when welding. Hence, the standard hardness of welding was found to be less important than the welding and parent metal excluding 90 % CMC metals welding.

2.3 Tensile Properties

The average tensile strength of welding by different CMC materials is shown in Fig. 7. It is observed that the 90 % CMC materials creates 20 N/mm² tensile strength. The tensile strength of 85 % CMC and 80 % CMC materials welding produce 68 N/mm² and 119.2 N/mm² respectively, which is superior to the 90 % CMC materials. It is observed that all wedding samples create the higher tensile strength than 90 % CMC in all factors of welding parameters due to the increasing of reinforcements [31]. The cross-sections of welding for different CMC materials are presented in Fig. 8.

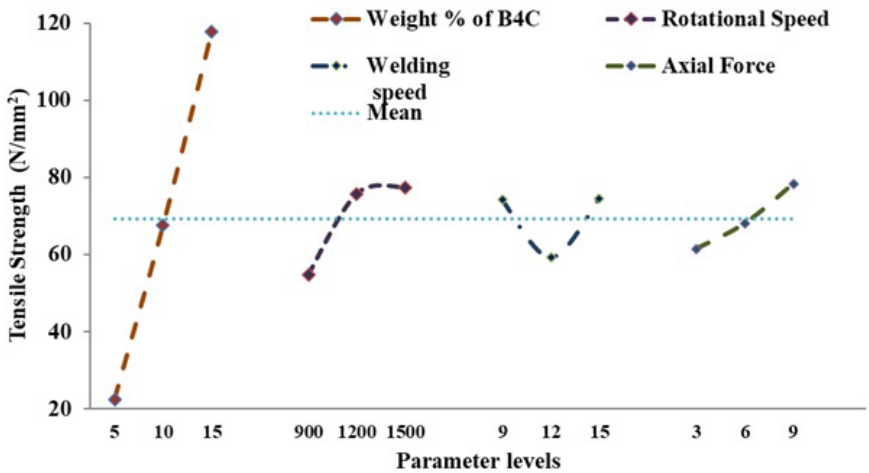

Fig. 7. *Tensile strength representation*

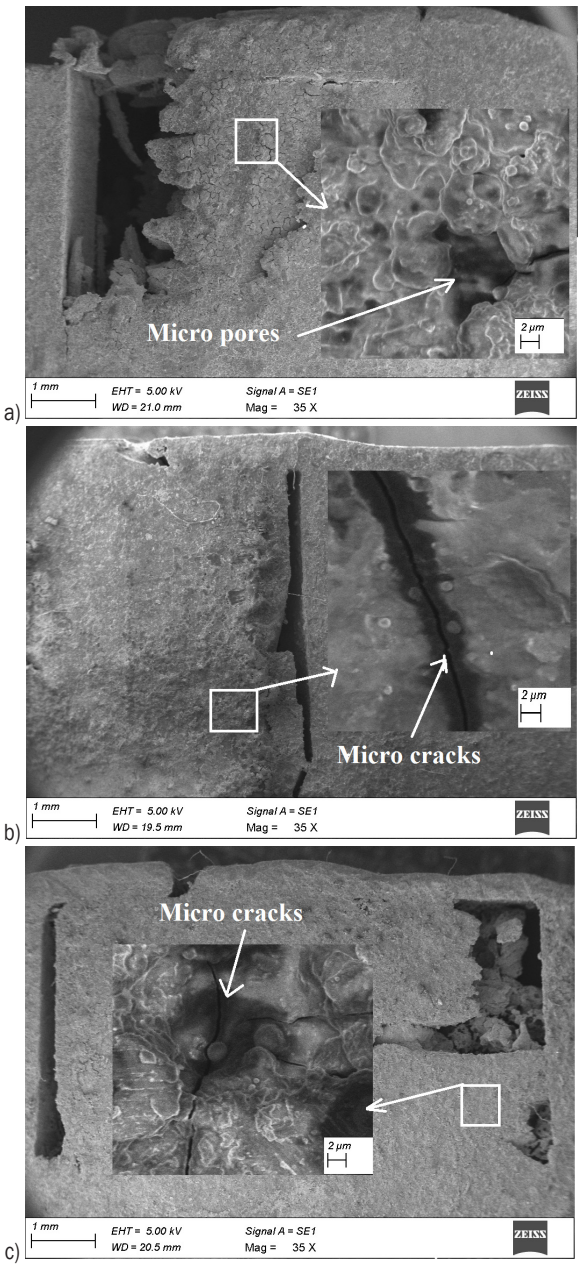

Fig. 8. *SEM image of welding cross-sections; a) 90 % CMC, b) 85 % CMC, and c) 80 % CMC*

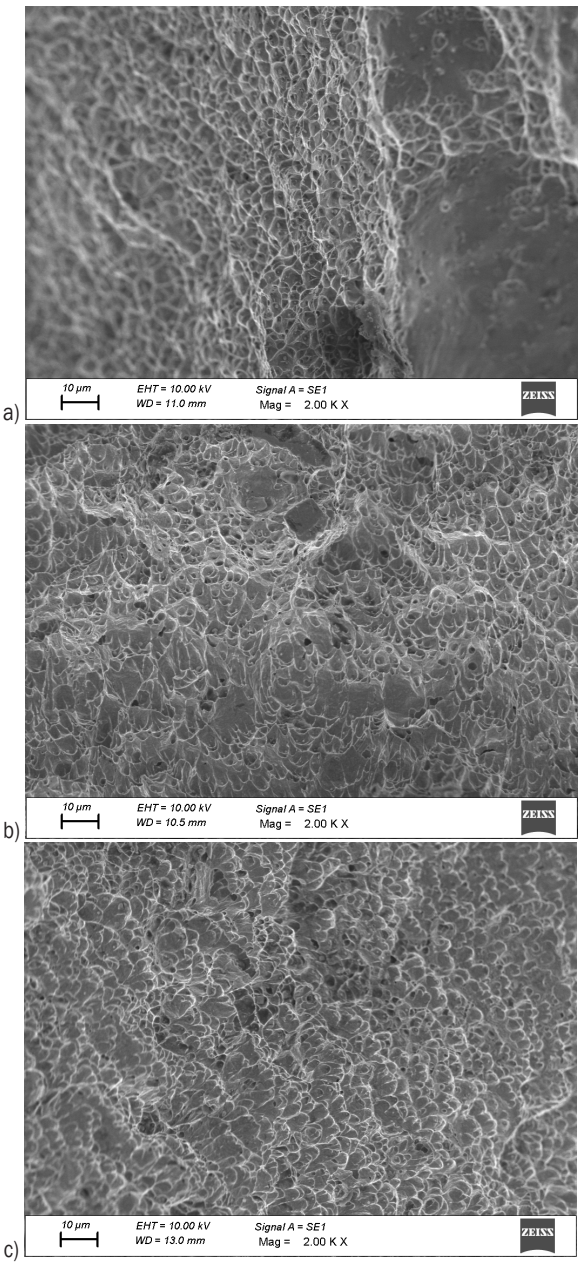

Fig. 9. *SEM image of fractured cross section; a) 90 % CMC, b) 85 % CMC, and c) 80 % CMC*

2.4 Impact Strength

Fig. 10 presents the impact strength for the different CMC welding samples under different parameter levels. It is apparent that addition of B_4C with CMC excites the creep strength in work material, which led to the elevated toughness. Of the various CMCs used as work material, the 80 % CMC work metal produces the maximum toughness of 4.39 J, and its cracked surface is shown in Fig. 9c. 80 % CMC work metal produces 68 % upper toughness than that using of welding on 90 % CMC work metal. The SEM image in Fig. 9a shows the broken surfaces with 80 % CMC work metal welding specimen. It is apparent from the image that the sample shows the cleavage surface and mild micro-dimples as seen through white marks [22]. The 85 % CMC work metal produces the second-highest impact toughness of 4.6 J among

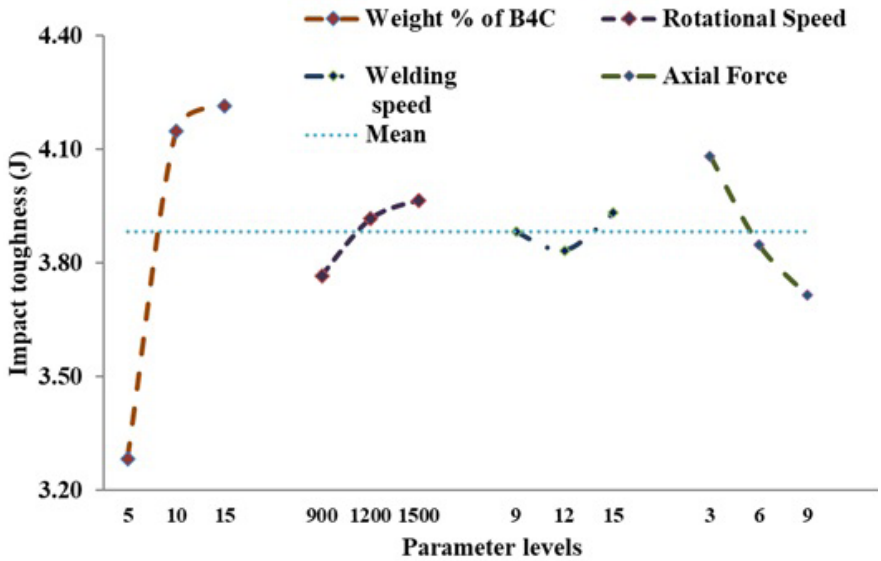

Impact strength of welding

others. Hence, 10 % B_4C added CMC work metal produces 53 % higher impact toughness compared to the 90 % CMC. Fig. 9b presents the broken surface of welding with 90 % CMC work metal. According to the Fig. 9, 90 % CMC work metal produces a stringy microstructure and micro-voids over the broken surface. This is due to the easy movement of B_4C from one side to another side by the tool revolutions.

2.5 TOPSIS

The outcome responses of FSW process (e.g., hardness, tensile and impact strength) for different CMC work materials are optimized through the TOPSIS method. The preference values of outcome responses are calculated using Eq. (1) to (8). The weights for the responses are assigned equally under ideal conditions. The ranking of experimentation is presented in Table 4. The outcome responses of the experimentation are transformed from multi-attribute optimization to single objective optimization using Taguchi's and TOPSIS method combination. The uppermost preference value (k_i) is considered the optimal parameter combination, and the highest rank is termed "first optimal solution". Consequently, it is observed that the 7th experimental run (0.8376 k_i value) is selected as the optimal parameter combination for the finest performance of FSW process. The experimental runs 2nd and 15th presents the next suitable optimal parameter solution. Therefore, the suitable optimal parameter combination is found to be that 15 % B_4C, 1200 rpm rotational speed, 9 mm/min welding speed and 9 kN axial force using TOPSIS.

Table 4. *TOPSIS ranking*

Experiment No.	T_i^+	T_i^-	Preference value, k_i	Rank
1	0.1749	0.3981	0.6948	4
2	0.1473	0.4558	0.7557	2
3	0.2588	0.3803	0.5950	7
4	0.2323	0.2910	0.5561	11
5	0.2484	0.2657	0.5168	12
6	0.2125	0.3041	0.5887	8
7	0.0869	0.4485	0.8376	1
8	0.4182	0.1156	0.2166	18
9	0.4523	0.1391	0.2352	17
10	0.1791	0.3938	0.6874	5
11	0.1829	0.3610	0.6636	6
12	0.2435	0.3410	0.5834	9
13	0.2173	0.2970	0.5775	10
14	0.2796	0.2366	0.4584	13
15	0.1594	0.3640	0.6954	3
16	0.3512	0.2487	0.4146	14
17	0.3857	0.1429	0.2703	15
18	0.4432	0.1521	0.2555	16

2.6 Table of ANOVA for TOPSIS

Analysis of variance (ANOVA) is the most suitable technique to find the significant and nonsignificant parameter from the experiments. The ki values of various CMC work material under different machining

conditions are mathematically studied using ANOVA method, and all individual parameter solution over the outcome responses are investigated. Furthermore, the *F*-test results are employed to find the most significant parameter to obtain the good performance measure. Table 5 makes apparent that composite work materials, i.e., the percentage of reinforcements with copper material contributes more impact on welding characteristics by around 43.89 %. Subsequently, the significant factor is axial force that produces 32.68 % contribution on the FSW process.

Table 5. *ANOVA for TOPSIS*

Symbol	Machining parameter	df	SS	MS	F	% contribution
A	Rc	2	0.2645	0.1322	37.54	43.89
B	Rs	2	0.0808	0.0404	11.48	13.42
C	Ws	2	0.0285	0.0143	4.05	4.73
D	Af	2	0.1969	0.0985	27.95	32.68
E	Error	9	0.0317	0.0035		5.28
	Total	17	0.6024	0.0354		100

2.7 GRA Method

The GRA method is a prominent technique employed to optimize the process parameters of the FSW process, such as micro-hardness, and tensile and impact strength. The GRC and GRG values are derived from Eqs. (11) and (12) for all experiments. The weights for the outcome responses are assigned equally (i.e., 1) and GRG values are presented in Table 6. The highest GRG value is selected as optimal parameter solution. Hence, the table suggest that the 7th experimental run (0.8465) holds the first rank and is termed as the optimal solution for better performance. The experimental combinations 2nd (0.8461) and 10th (0.8226) have the next best optimal parameter combination using the GRA method. Therefore, the suitable and optimal parameter combination found to be that 15 % B_4C, 1200 rpm rotational speed, 9 mm/min welding speed and 9 KN axial force using GRA.

2.8 ANOVA for GRG

The results obtained from the GRG for the various parameter combinations are analysed mathematically using ANOVA, which is presented in Table 7. The GRA approach is used to optimize the obtained results for different CMC materials. According to this, the percentage of reinforcements in work materials affects the welding performances significantly at about 37.85 %. The axial force of welding tool creates impact on the welding performance around 33.22 %, which is the next significant factor in the FSW process.

Table 6. *GRG ranking*

Experiment No.	GRC			GRG	Rank
	Hardness	Tensile strength	Impact toughness		
1	0.6022	0.8890	0.8333	0.7748	4
2	0.6292	1.0000	0.9091	0.8461	2
3	0.5000	0.8778	0.7692	0.7157	7
4	0.7943	0.6711	0.6250	0.6968	10
5	0.7134	0.6645	0.6452	0.6743	13
6	0.7467	0.7070	0.6061	0.6866	11
7	1.0000	0.8729	0.6667	0.8465	1
8	0.6087	0.5309	0.6452	0.5949	17
9	0.6627	0.5000	0.6897	0.6175	15
10	0.5989	0.8689	1.0000	0.8226	3
11	0.6222	0.8257	0.7143	0.7207	6
12	0.5333	0.8011	0.8696	0.7347	5
13	0.7467	0.6929	0.6667	0.7021	9
14	0.6667	0.6509	0.5556	0.6244	14
15	0.7368	0.8015	0.6061	0.7148	8
16	0.9256	0.5610	0.5556	0.6807	12
17	0.6437	0.5506	0.6061	0.6001	16
18	0.7179	0.5092	0.5000	0.5757	18

Table 7. *ANOVA table for GRG*

Symbol	Machining parameter	df	SS	MS	F	% contribution
A	Ce	2	0.0438	0.0219	0.00825191	37.85
B	Vm	2	0.0246	0.0123	68.1870725	21.30
C	Cd	2	0.0072	0.0036	19.9226318	6.22
D	Te	2	0.0384	0.0192	106.335841	33.22
E	Error	9	0.0016	0.0002		1.41
	Total	17	0.1157	0.0068		100

3 CONCLUSIONS

This paper attempted to express the advantages and performance study of FSW process with copper composite material in reinforcement addition. Three CMC materials are prepared using pure copper (Cu) as the matrix; tungsten (W) and boron carbide (B_4C) particles are reinforcements for various concentrations. The multi-objective decision-making methods, such as TOPSIS and GRA methods are used to find the optimal parameter combination, and experiments are planned according to the L 18 orthogonal array (OA), using the most influential parameters, such as the percentage of boron carbide

reinforcements, tool rotational speed, welding speed, and axial force.

- Based on the optimization results, 15 % of B_4C, 900 rpm rotational speed, 15 mm/min welding speed and 6 kN axial forces produces the better mechanical strength on the welding using both TOPSIS and GRA techniques.
- The microstructure of welding reveals that consistency of welding joint on all sides of the parent metal is found to be better in 15 % B_4C reinforced CMC materials than other reinforced work materials, and lesser regularity found in 5 % B_4C reinforced CMC material.
- 80 % CMC and 85 % CMC reinforced copper work metal produces 68 % and 10 % higher impact toughness respectively than that using of welding on 90%CMC work metal.
- Based on the ANOVA table of TOPSIS, composite work materials, the percentage of reinforcements with copper material contributes more impact on welding characteristics of around 43.89 %. Subsequently, the next significant factor is axial force, which produces a 32.68 % contribution on the FSW process.
- Therefore, the mechanical strength of welding with FSW process increases with an increase of the percentage of reinforcement in the copper composite material. Also, these types of materials could be used for the applications for which high mechanical strength is required.
- Furthermore, experiments with hybrid composite with pure copper can be conducted, and assistance with FSW process such as heat energy can be experimentally tested with the FSW process to enhance the welding quality.

4 REFERENCES

[1] Zamani, S.M.M., Behdinan, K., Razfar, M.R., Fatmehsari, D.H., Mohandesi, J. A. (2021). Studying the effects of process parameters on the mechanical properties in friction stir welding of Al-SiC composite sheets. *The International Journal of Advanced Manufacturing Technology*, vol. 113, p. 3629-3641, **DOI:10.1007/s00170-021-06852-7**.

[2] Bakhtiari Argesi, F., Shamsipur, A., Mirsalehi, S.E. (2021). Preparation of bimetallic nano-composite by dissimilar friction stir welding of copper to aluminum alloy. *Transactions of Nonferrous Metals Society of China*, vol. 31, no. 5, p. 1363-1380, **DOI:10.1016/S1003-6326(21)65583-8**.

[3] Sudhagar, S., Gopal, P.M. (2022). Investigation on mechanical and tribological characteristics Cu/Si3N4 surface composite developed through friction stir processing. *Silicon*, vol. 14, p. 4207-4216, **DOI:10.1007/s12633-021-01206-0**.

[4] Thapliyal, S., Mishra, A. (2021). Machine learning classification-based approach for mechanical properties of friction stir welding of copper. *Manufacturing Letters*, vol. 29, p. 52-55, **DOI:10.1016/j.mfglet.2021.05.010**.

[5] Harisha, P., Nanjundaswamy, H.M., Divakar, H.N., Krishnan, D. (2022). Tensile properties of aluminium and copper alloys friction stir welded joints. *Materials Today: Proceedings*, vol. 54, p. 223-227, **DOI:10.1016/j.matpr.2021.08.297**.

[6] Nagesh, G., Rao, K.N., Anurag, K.M., Abhinav, N. (2021). Investigation of mechanical properties on non-ferrous alloys of copper and brass joints made by friction stir welding. *IOP Conference Series: Materials Science and Engineering*, vol. 1057, no. 1, art. ID 012062, **DOI:10.1088/1757-899X/1057/1/012062**.

[7] Senthil, S.M., Parameshwaran, R., Nathan, S.R., Kumar, M.B., Deepandurai, K. (2020). A multi-objective optimization of the friction stir welding process using RSM-based-desirability function approach for joining aluminum alloy 6063-T6 pipes. *Structural and Multidisciplinary Optimization*, vol. 62, p. 1117-1133, **DOI:10.1007/s00158-020-02542-2**.

[8] Karrar, G., Galloway, A., Toumpis, A., Li, H., Al-Badour, F. (2020). Microstructural characterisation and mechanical properties of dissimilar AA5083-copper joints produced by friction stir welding. *Journal of Materials Research and Technology*, vol. 9, no. 5, p. 11968-11979, **DOI:10.1016/j.jmrt.2020.08.073**.

[9] Kolnes, M., Kübarsepp, J., Sergejev, F., Kolnes, M., Tarraste, M., Viljus, M. (2020). Performance of ceramic-metal composites as potential tool materials for friction stir welding of aluminium, copper and stainless steel. *Materials*, vol. 13, no. 8, art. ID 1994, **DOI:10.3390/ma13081994**.

[10] Sahu, P.K., Pal, S., Das, B., Shi, Q. (2020). Fabrication and effect of Mg-Zn solid solution via Zn foil interlayer alloying in FSW process of magnesium alloy. *Archives of Civil and Mechanical Engineering*, vol. 20, art. ID 137, **DOI:10.1007/s43452-020-00141-y**.

[11] Jimenez-Mena, N., Jacques, P. J., Ding, L., Gauquelin, N., Schryvers, D., Idrissi, H., Simar, A. (2019). Enhancement of toughness of Al-to-steel friction melt bonded welds via metallic interlayers. *Materials Science and Engineering: A*, vol. 740-741, p. 274-284, **DOI:10.1016/j.msea.2018.10.101**.

[12] Garg, A., Bhattacharya, A. (2019). Influence of Cu powder on strength, failure and metallurgical characterization of single, double pass friction stir welded AA6061-AA7075 joints. *Materials Science and Engineering: A*, vol. 759, 661-679, **DOI:10.1016/j.msea.2019.05.067**.

[13] D D'Souza, A., Rao, S.S., Herbert, M.A. (2019). Assessment of influence of process parameters on properties of friction stir welded Al-Ce-Si-Mg aluminium alloy. *Materials Research Express*, vol. 6, no. 8, art. ID 086504, **DOI:10.1088/2053-1591/ab1aec**.

[14] Shettigar, A.K., Herbert, M.A., Rao, S. S. (2019). Microstructure evolution and mechanical properties of friction stir welded AA6061/rutile composite. *Materials Research Express*, vol. 6, art. ID 0865i7, **DOI:10.1088/2053-1591/ab0f4e**.

[15] Khojastehnezhad, V.M., Pourasl, H.H. (2018). Microstructural characterization and mechanical properties of aluminum 6061-T6 plates welded with copper insert plate (Al/Cu/Al) using friction stir welding. *Transactions of Nonferrous Metals*

Society of China, vol. 28, no. 3, p. 415-426, **DOI:10.1016/S1003-6326(18)64675-8**.

[16] Babu, K.K., Panneerselvam, K., Sathiya, P., Haq, A.N., Sundarrajan, S., Mastanaiah, P., Murthy, C.S. (2018). Parameter optimization of friction stir welding of cryorolled AA2219 alloy using artificial neural network modeling with genetic algorithm. *The International Journal of Advanced Manufacturing Technology*, vol. 94, p. 3117-3129, **DOI:10.1007/s00170-017-0897-6**.

[17] Peddavarapu, S., Raghuraman, S., Bharathi, R.J., Sunil, G.V.S., Manikanta, D.B.N.S. (2017). Micro structural investigation on friction stir welded Al-4.5Cu-5TiB2 Composite. *Transactions of the Indian Institute of Metals*, vol. 70, p. 703-708, **DOI:10.1007/s12666-017-1072-3**.

[18] Herbert, M.A., Shettigar, A.K., Nigalye, A.V., Rao, S.S. (2016). Investigation on microstructure and mechanical properties of friction stir welded AA6061-4.5Cu-10SiC composite. *IOP Conference Series: Materials Science and Engineering*, vol. 114, no. 1, art. ID. 012125, **DOI:10.1088/1757-899X/114/1/012125**.

[19] Sahu, P.K., Kumari, K., Pal, S., Pal, S.K. (2016). Hybrid fuzzy-grey-Taguchi based multi weld quality optimization of Al/Cu dissimilar friction stir welded joints. *Advances in Manufacturing*, vol. 4, p. 237-247, **DOI:10.1007/s40436-016-0151-8**.

[20] Ahmadkhaniha, D., Heydarzadeh Sohi, M., Zarei-Hanzaki, A., Bayazid, S.M., Saba, M. (2015). Taguchi optimization of process parameters in friction stir processing of pure Mg. *Journal of Magnesium and Alloys*, vol. 3, no. 2, p. 168-172, **DOI:10.1016/j.jma.2015.04.002**.

[21] Shirazi, H., Kheirandish, S., Safarkhanian, M.A. (2015). Effect of process parameters on the macrostructure and defect formation in friction stir lap welding of AA5456 aluminum alloy. *Measurement*, vol. 76 p. 62-69, **DOI:10.1016/j.measurement.2015.08.001**.

[22] Kumar, A., Veeresh Nayak, C., Herbert, M.A., Rao, S.S. (2014). Microstructure and hardness of friction stir welded aluminium-copper matrix-based composite reinforced with 10 wt-% SiCp. *Materials Research Innovations*, vol. 18, S6-84-S6-89, **DOI:10.1179/1432891714Z.0000000001016**.

[23] Suresh, S., Natarajan, E., Franz, G., Rajesh, S. (2022). Differentiation in the SiC filler size effect in the mechanical and tribological properties of friction-spot-welded AA5083-H116 alloy. *Fibers*, vol. 10, no. 12, art. ID 109, **DOI:10.3390/fib10120109**.

[24] Suresh, S., Elango, N., Venkatesan, K., Lim, W.H., Palanikumar, K., Rajesh, S. (2020). Sustainable friction stir spot welding of 6061-T6 aluminium alloy using improved non-dominated sorting teaching learning algorithm. *Journal of Materials Research and Technology*, vol. 9, no. 5, p. 11650-11674, **DOI:10.1016/j.jmrt.2020.08.043**.

[25] Suresh, S., Venkatesan, K., Natarajan, E., Rajesh, S. (2020). Performance analysis of nano silicon carbide reinforced swept friction stir spot weld joint in AA6061-T6 alloy. *Silicon*, vol. 13, p. 3399-3412, **DOI:10.1007/s12633-020-00751-4**.

[26] Suresh, S., Natarajan, E., Shanmugam, R., Venkatesan, K., Saravanakumar, N., Anto Dilip, A. (2022). Strategized friction stir welded AA6061-T6/SiC composite lap joint suitable for sheet metal applications. *Journal of Materials Research and Technology*, vol. 21, p. 30-39, **DOI:10.1016/j.jmrt.2022.09.022**.

[27] Soundarrajan, M., Thanigaivelan, R. (2018). Investigation on electrochemical micromachining (ECMM) of copper inorganic material using UV heated electrolyte. *Russian Journal of Applied Chemistry*, vol. 91, p. 1805-1813, **DOI:10.1134/S1070427218110101**.

[28] Soundarrajan, M., Thanigaivelan, R. (2019). Investigation of electrochemical micromachining process using ultrasonic heated electrolyte. *Advances in Micro and Nano Manufacturing and Surface Engineering*, p. 423-434. Springer, Singapore, **DOI:10.1007/978-981-32-9425-7_38**.

[29] Saravanan, K.G., Thanigaivelan, R., Soundarrajan, M. (2021). Comparison of Electrochemical Micromachining Performance using TOPSIS, VIKOR and GRA for Magnetic field and UV rays heated Electrolyte. *Bulletin of the Polish Academy of Sciences, Technical Sciences*, vol. 69, no. 5, **DOI:10.24425/bpasts.2021.138816**.

[30] Soundarrajan, M., Thanigaivelan, R. (2017). Intervening variables in electrochemical micro machining for copper. *International Conference on Precision, Meso, Micro and Nano Engineering*, p. 263-266.